Torque Ripple Minimization in Switch Reluctance Motor Using Model Predictive Control for Water Pumping Application

**Aguemon Dourodjayé Pierre[1], Agbokpanzo Richard Gilles[2*],
Houngan Kokou Théophile[1] and Vianou Antoine[1]**

[1]*University of Abomey-Calavi, EPAC, Benin.*
[2]*University of Abomey, UNSTIM/ENSET-Lokossa, Benin.*

Authors' contributions

*This work was carried out in collaboration between all authors. All authors read and approved the
final manuscript.*

Original Research Article

Abstract

This paper presents the torque ripple minimization in switched reluctance motor (SRM) for water
pumping. The model predictive control (MPC), one of the rugged control, is used to minimize this
torque ripple. According to the receding horizon, the MPC predicted the behavior of the system
by generating the control signal to minimize the torque ripple. At each sampling time, an optimal
control for torque ripples minimization is elaborated and only the first element is applied to the
system according to the receding horizon control. The MPC minimized the real stator currents
to reach the objective. The simulations on Matlab demonstrated that a very low rate of ripples
could be obtained by setting the parameters of the MPC indicating the high potential of MPC in the
control of SRM.

*Corresponding author: E-mail: richgille@gmail.com

1   INTRODUCTION

Pumping is an ideal solution for supply in water.   A pumping system consists of an electric motor with its power supply and a pump. The first motors used are the Induction motors and conventional DC motors. A Study of these two types of motors is reported in [1, 2, 3, 4].   Later on, the DC brushless motors with permanent magnet appeared in order to avoid the use of conventional DC motors [5, 6]. SRM, according to technological advanced in power electronics, emerged. Their construction price is reduced(52% of the price of the asynchronous motor and only 30% compared to the permanent magnet synchronous motor) and a reduced weight (85% of the weight of the magnet motor and 73% of the weight of the asynchronous motor) [7].   Their integration in pumping would be an adequate solution because of their robustness, reliability, competitive cost, simplicity, high torque compared to inertia, easy control, good efficiency and high speed operating capacity [8, 9].   The major disadvantage of this type of motor is that its torque ripples and is often accompanied by background noise and mechanical vibrations. This ripple shall be maintained within the permissible limits because it is not tolerable in direct drive applications [8].   According to literature, there are many approaches to reduce the torque ripples.   One used the torque sharing function based on the hysteresis control or pulse width modulation [8, 10, 11].   One used the hysteresis torque regulator to generate the demand stator current to minimize the torque ripple [12].   The above mentioned methods contributed to reduce the torque ripple. In this work, a different approach is pursued.   The MPC is used to control the torque minimization. The MPC control has been successfully used in several industrial control applications.   It is suitable for several industrial applications especially in power electronics such as converters DC-DC, DC-AC [13]. The approach used is, from the model of SRM, to determine the opening and closing angle of asymmetric bridge to minimize the currents that fed each phase of

the motor according to the information on the MPC input.   At each sample time, a torque is predicted according to the receding horizon. The stator currents are determined using the objective function.

2   MATERIALS AND METHODS

The rotor of SRM is made of steel lamination without coils or magnets.   The diametrically opposed stator windings are connected in series or in parallel to form an independent phase. The rotor is aligned when all the stator poles are excited [14]. A three-phase structure is presented in Fig. 1.

In this paper, we study a three phase SRM for which the electrical schematic diagram per phase is shown in Fig. 2.

On this figure $v(t)$ is the applied voltage, R the resistance of a winding, and $L(i, \theta)$ the variable inductance depending on the instantaneous position of the rotor θ and the current of the stator $i(t)$.   It is assumed for all three phases that the electrical resistances are identical, the inductances are identical and the poles of the rotor rotate at the same speed. The stator voltage is given by equation 2.1.

$$v(t) = Ri(t) + \frac{\partial \phi}{\partial i(t)} \frac{di(t)}{dt} + \omega \frac{\partial \phi}{\partial i(t)} \qquad (2.1)$$

The mechanical load is a centrifugal pump.   Its characteristic is given by the relationship:

$$T_L(t) = k\omega^2(t) \qquad (2.2)$$

where k is the constant and $\omega(t)$ the centrifugal pump speed. Considering that in addition to the centrifugal main torque, the load has an inertia J and a viscous torque proportional to the speed, the load equation is described by equation 2.3. [15, 16, 17, 18].

$$T_e(t) = J\frac{d\omega(t)}{dt} + f\omega(t) + T_L(t) \qquad (2.3)$$

To sum up and for a phase p, we obtain the SRM equation in state form.

$$\begin{cases} \frac{di_a(t)}{dt} = \frac{1}{\frac{\partial \Phi_a(i_p(t),\theta_p(t))}{\partial i_p(t)}} v(t) - Ri_p(t) - \omega_p(t)\frac{\partial \Phi_p(i_p(t),\theta_p(t))}{\partial \theta_p(t)} \\ \\ \frac{d\omega}{dt} = \frac{1}{J}T_e(t) - f\omega(t) \\ \\ \frac{d\theta}{dt} = \omega(t) \end{cases} \tag{2.4}$$

The Control strategy adopted in this work is shown in Fig. 3.
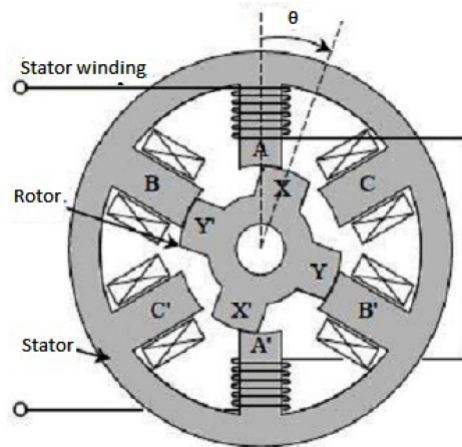
**Fig. 1. A three phase structure of the SRM**
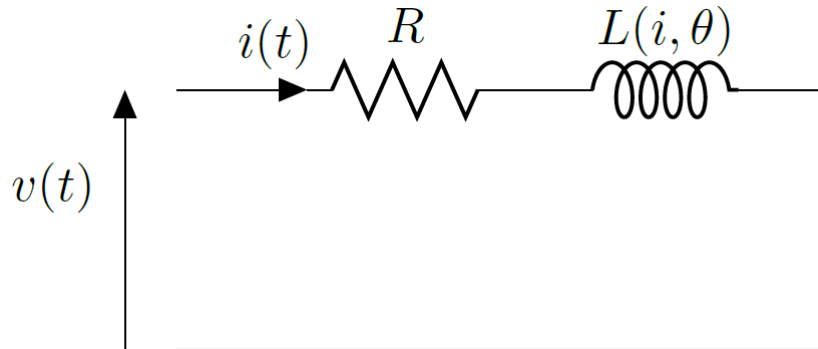
Fig. 2. Electrical diagram per phase

The reference speed ω_{ref} is compared to the instantaneous speed ω of the motor measured by the position sensor. The error ω_e is introduced in the speed regulator block to generate the reference or demanding torque Te_{ref}. The MPC command then predict the torque of the machine by taking into account the reference torque according to the principle of the

prediction horizon. It develops commands for this purpose, which are in this case reference stator currents I_{1ref}, I_{2ref} et I_{3ref}. These reference currents are introduced into the hysteresis current regulator block. The hysteresis current regulator generates at its output the switching times of each switch of the asymmetrical bridge. The asymmetric bridge then delivers the actual currents to the stator of the SRM at determined positions of the rotor. Fig. 4 present a typical structure of a model predictive control [19].

The two components of the prediction are the free response which shows the expected behavior of the system output $y(t+j)$ assuming future values of the control variables are equaled to zero and the forced response which forms the additional component of the system response based on the precalculated set of future control values $u(t+j)$.

The used parameters in the predictive control are N_p the prediction horizon N_c the horizon of control and r_w the weight. These parameters are obtained after several simulation for ajusting of

the response.

3   STATISTICAL METHODS

The SRM equations are linearized around the maximum point and the result is given in equation 3.1.

$$\begin{cases} x(k+1) = Ax(k) + Bu(k) \\ y(k) = Cx(k) \end{cases} \tag{3.1}$$

Where $x(k) = \begin{bmatrix} I_1 \\ I_2 \\ I_3 \\ \omega \\ \theta \\ T_e \end{bmatrix}$ is the state vector, $u(k) = \begin{bmatrix} I_{1ref} \\ I_{2ref} \\ I_{3ref} \end{bmatrix}$ the control vector and $y(k)$ the output.

The state, control and observability matrices are given by:

$$A = \begin{bmatrix} -\frac{R}{a} & 0 & 0 & -\frac{b}{a} & 0 & 0 \\ 0 & -\frac{R}{a} & 0 & -\frac{b}{a} & 0 & 0 \\ 0 & 0 & -\frac{R}{a} & -\frac{b}{a} & 0 & 0 \\ 0 & 0 & 0 & (k\omega^2 + f)/J & 0 & 0 \\ 0 & 0 & 0 & 1 & 0 & 0 \\ 0 & 0 & 0 & 0 & 1 & T_{emax} \end{bmatrix}$$

$$B = \begin{bmatrix} \frac{1}{a} & 0 & 0 \\ 0 & \frac{1}{a} & 0 \\ 0 & 0 & \frac{1}{a} \\ 0 & 0 & 0 \\ 0 & 0 & 0 \\ 0 & 0 & 0 \end{bmatrix}$$

and

$$C = [0\ 0\ 0\ 0\ 0\ 1]$$

The linearized model was made considering two positions of the rotor. The aligned position in which $\theta = 0°$ and the flux is a non-linear function and unaligned position in which $\theta = 45°$ and the flux is a linear function [20]. The flux and torque are evaluated.

$$\Phi_p(i_p, \theta_p) = L_q i_q + \left[L_{dsat} i_q + A(1 - e^{-Bi_p}) - L_q i_q \right] f(\theta)$$
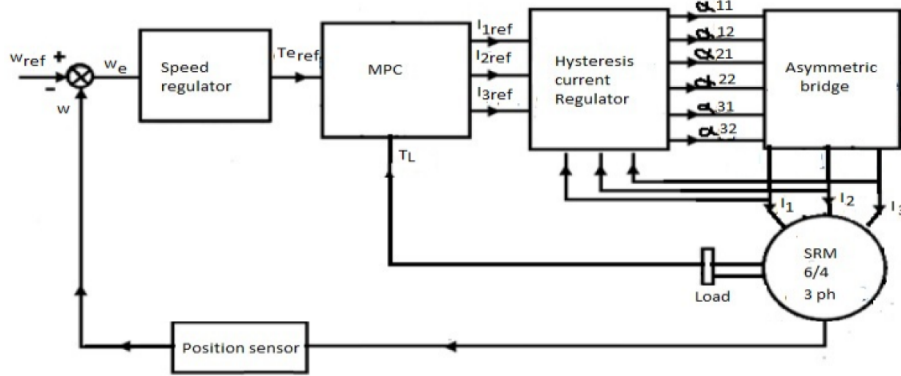
Fig. 3. Control strategy
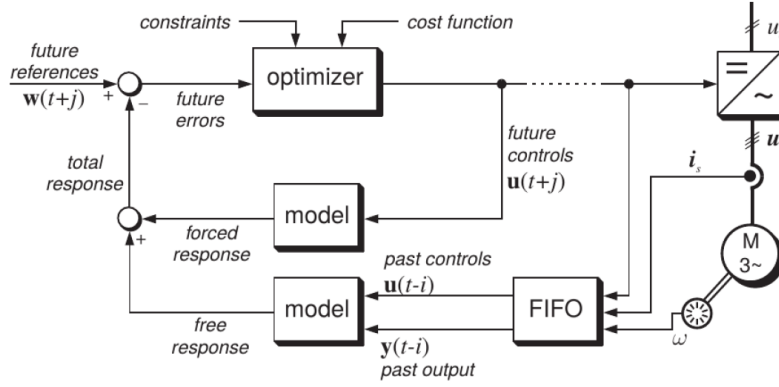
Fig. 4. Typical structure of an MPC controller

$$T_{e,p}(i_p, \theta_p) = \left[\frac{L_{dsat} - L_q}{2} i_q^2 + A i_q - \frac{A}{B}(1 - e^{-B i_p}) f'(\theta) \right]$$

Where $f(\theta_p) = \begin{cases} \frac{128\theta_p^3}{\pi^3} \frac{48\theta_p^2}{\pi^2} + 1 \text{ if } \theta_p \in [0 \ \pi/4] \\ \\ f(\pi/2 - \theta_p) \text{ if } \theta_p \in [\pi/4 \ \pi/2] \end{cases}$

A and B are constants calculated from the maximum point. The maximal point parameters are $I_m = 450A$, $\theta_m = 15°$ and $\Phi_m = 0.468Wb$.

4 RESULTS AND DISCUSSION

The parameters of the centrifugal pump and the used motor are presented in Table 1.

The closed loop diagram of the torque control in Matlab is shown in Fig. 5. The simulation was done at the reference rated torque and at the half of the rated torque. The MPC block is shown in Fig. 6.

Table 1. MRV and centrifugal pump parameters

| Parameters	Value
Power	$6kW$
Speed	$1500rpm$
Number of phase	3
Pole per phase of stator	6
Pole per phase of rotor	4
Resistance of stator R_s	0.72Ω
Direct inductance L_d	$23.62mH$
Quadrature inductance L_q	$0.67mH$
Moment of inertia J	$0.008kg.m^2$
Friction coefficient f	$0.02N.m.s/rad$
Centrifugal pump parameter k	0.0015
Motor's rated torque $T_{e,nm}$	$41.339N$
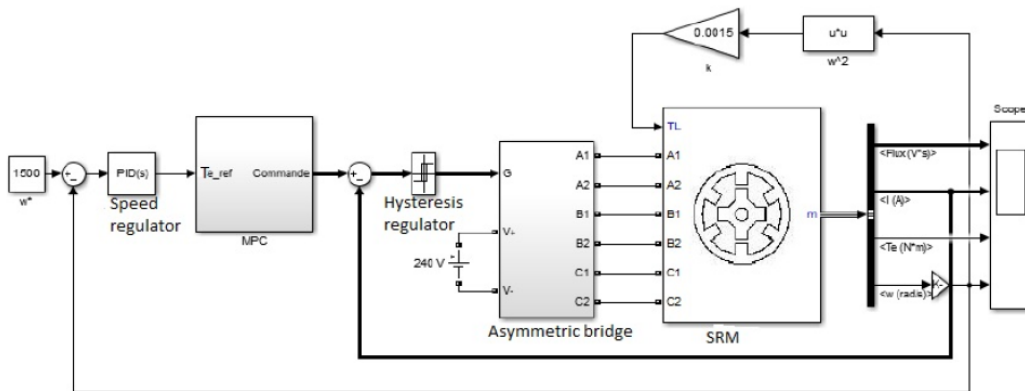
Fig. 5. Closed loop diagram of the system

This block takes as in its input the reference torque Te_{ref} and evaluates the control signal using the state, control and observability matrices. The error between the input and the output is then evaluated to reach to the goal.

Fig. 7 shows the torque control result at the left and the zoom of the transient response at the right.

The speed of the motor is shown in Fig. 8. The motor's working at the rated torque is presented at the left and its working for a half rated torque at the right.

For the rated working, the SRM developed high torque during the transient regime. The steady state is reached after a response time of 0.35 milliseconds. The ripples are attenuated in this steady state. The MPC parameters have been set to $N_p = 3$, $N_c = 2$ and $r_w = 0.05$. Concerning the working at the $1060.7r/min$, the motor operated at half its rated torque of $20.669N.m$. The torque response time for a reference of $20.669N.m$ is 0.28 milliseconds. This time is better than that of nominal operation. However, a good setting of the MPC control can guarantee a better response time.

The resulting torque response is related to the correct parameterization of the MPC command. This response is obtained after several simulation
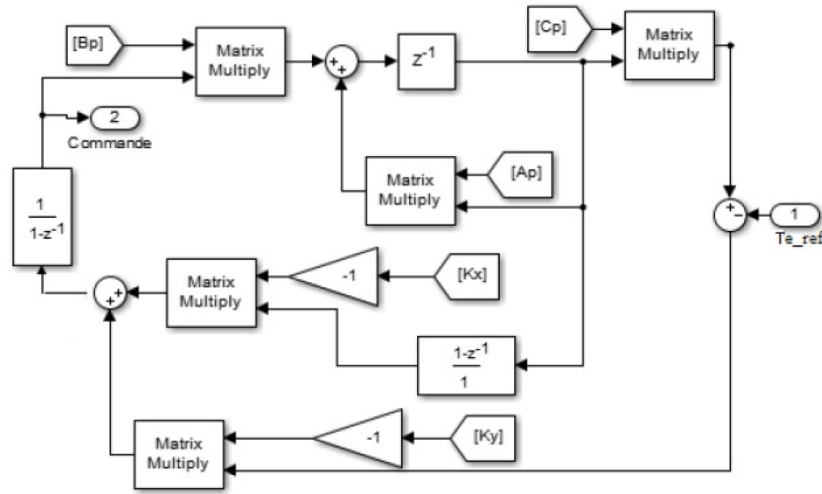
Fig. 6. Implementing of the MPC bloc in SIMULINK
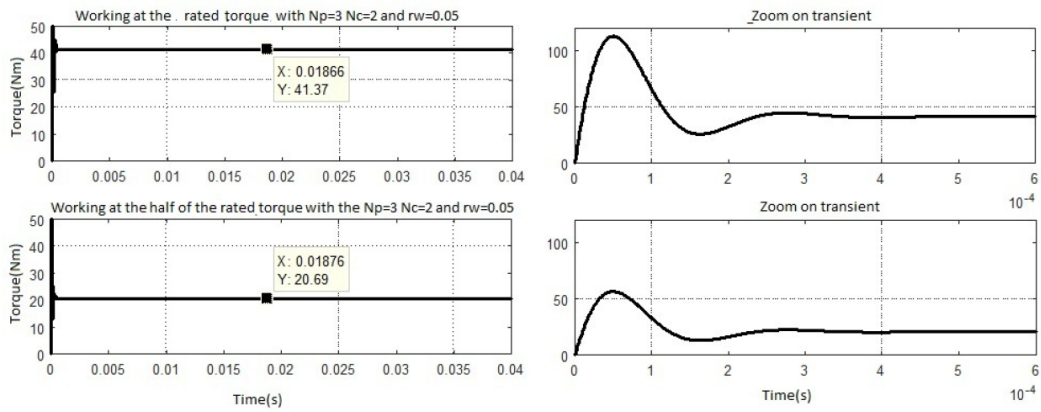
Fig. 7. Torque control
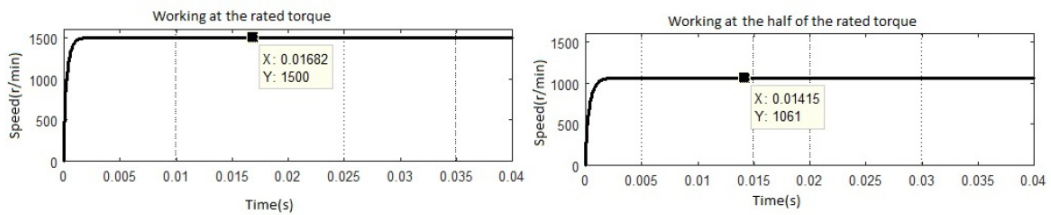
Fig. 8. Speed of the motor with different value of torque

tests mainly for the choice of N_p and N_c guaranteeing a good response time. The torque and speed regulated in both operating steady state are without ripples. The same result was

found in [21, 22, 23, 24, 25] using the SEPIC converter and others. The difference in this work is to avoid the use of a converter that can make the water pumping system costly. The result obtained is also due to the choice of the model used and the parameters of the maximum point for the linearization.

5 CONCLUSION

This work was carried out within the framework of the minimization of the torque ripples in Switched Reluctance Motor for water pumping. The method used consists in applying the MPC command to reduce the torque ripples at the lower level.

From this work, we found that the MPC command allows to avoid the use of a converter which can make costly the water pumping system.

COMPETING INTERESTS

Authors have declared that no competing interests exist.

References

[1] Aicha Znidi, Said Chniba, Emna Bouazizi. Etude d'une installation de pompage solaire à moteur à courant continu. 2ème conférence Internationale des énergies renouvelables CIER. 2014;3:116-122.

[2] Abdelmalek Mokeddem, et al. Test and analysis of a photovoltaic dc-motor pumping system. ICTON-MW. 2007;1-7.

[3] Brahmaiah B, Venkateswra rao Ch., Tulasiram SS. PVG based smart energy modeling for agricultural sector. International Journal of Electrical Engineering and Technology. 2013;4(2):1-9.

[4] Ahmed M. Kassem, Ali M.Yousef. Fuzzy-logic based self-tuning pi controller for high-performance vector controlled induction motor fed by pv-generator. Journal of Engineering Sciences. 2012;40(4):1-13.

[5] Bhim Singh, Rajan Kumar. Solar photovoltaic array fed water pump driven by brushless dc motor using landsman converter. IET Renewable Power Generation. 2015;1-11.

[6] Loïc Quéval, et al. Photovoltaic motors review, comparison and switched reluctance motor prototype. Tenth International Conference on Ecological Vehicles and Renewable Energies (EVER). 2015;1-8

[7] David G. Dorell, et al. Comparison of different motor design drives for hybrid electric vehicles. Energy Conversion Congress and Exposition ECCE, Atlanta, GA. 2010;3352-3359.

[8] Jebarani Evangeline S, et al. Minimization of torque ripple in switched reluctance motor drive: A review. Advanced Electrical and Electronics Engineering. LNEE. 2011;87:287-294.

[9] Moussi A, Betka A. Rendement maximis d'un moteur asynchrone aliment par une source photovoltaque. Larhyss Journal, ISSN 1112-3680. 2003;2:1-10.

[10] Jin Ye, et al. An offline torque sharing function for torque ripple reduction in switched reluctance motor drives. IEEE Transactions on Energy Conversion, 0885-8969; 2015.

[11] Stella K, Nisha GK. State of the art of switched reluctance motor for torque ripple minimization. International Journal of Industrial Electronics and Electrical Engineering. 2014;2(12).

[12] Srinivas P, Prasad PVN. Torque ripple minimization of 4 phase 8/6 switched reluctance motor drive with direct instantaneous torque control. International Journal on Electrical Engineering and Informatics. 2014;3(4):488-497

[13] Villegas J, et al. Model predictive control of a switched reluctance machine using discrete space vector modulation. 978-1-4244-6392-3/10 IEEE; 2010.

[14] Amissa Arifin, et al. State of the art of switched reluctance generator, energy and power engineering. EEE. 2012;1-12.

[15] Gupta Rajesh Kumar RA, Bishnoi SK. Modeling and control of nonlinear switched reluctance motor drive. Journal of Electrical Engineering; 2011.

[16] Radim Visinka. 3-phase switched reluctance sensorless motor control using a 56f80x, 56f8100 or 56f8300 device. Freescale Semiconductor, Rev. 2

[17] Mousavi-Aghdam SR. A new method to reduce torque ripple in switched reluctance motor using fuzzy sliding mode. Iranian Journal of Fuzzy Systems. 2012;9(1):1-12

[18] Anjanee Kumar Mishra, Bhim Singh. Control of SRM drive for photovoltaic powered water pumping system. IET Electric Power Applications. 2017;11(6):1055-1066.

[19] Arne Linder, Rahul Kanchan, Ralph Kennel, Peter Stolze. Model-based predictive control of electric drives. Book, Munich, June 2010.

[20] Le-Huy H, Brunelle P. A versatile nonlinear switched reluctance motor model in simulink using realistic and analytical magnetization characteristics. 31st Annual Conference of IEEE. 2005;1556-1561.

[21] Sweta Belliwali, et al. Mathematical modelling and simulation of directly coupled pv water pumping system employing switched reluctance motor. IEEE PES Innovative Smart Grid Technologies, India. 2011;1-5.

[22] Quéval L, et al. Photovoltaic switched reluctance motor modeling and simulation. 978-1-4799-7993-6/15 IEEE; 2015.

[23] Singh S, Anjanee Kumar Mishra. Performance of solar photovoltaic array fed water pumping system utilizing switched reluctance motor. International Journal of Engineering, Science and Technology, Joint International Conference. 2015;7:1-9.

[24] Singh S, Anjanee Kumar Mishra. Canonical switching cell converter fed srm drive for spy array based water pumping. 978-9-3805-4416-8/15 IEEE

[25] Singh S, et al. Solar powered water pumping system employing switched reluctance motor drive. IEEE Transactions on Industry Applications, 0093-9994 (c)